ADVANCES IN MATERIALS SCIENCE, Vol. 23, No. 2 (76), June 2023

DOI: 10.2478/adms-2023-0010

Arezki Sarri[1], Mehena Oualit[2*], Salim Kennouche[3]

[1]*Laboratory of Polymers Treatment & Forming, M'Hamed Bougara University, Boumerdes, Algeria*
[2]*Research Unit: Materials, Processes and Environment (UR-MPE), Faculty of Technology, M'hamed Bougara University, Boumerdes, Algeria*
[3]*Department of Civil Engineering, Faculty of Sciences, Bouira University, Algeria*

** m.oualit@univ-boumerdes.dz*

VALORIZATION OF A STEEL INDUSTRIAL CO-PRODUCT FOR THE DEVELOPMENT OF ALKALI-ACTIVATED MATERIALS: EFFECT OF CURING ENVIRONMENTS

ABSTRACT

While natural resources are becoming scarce and climate change is accelerating, the recovery and recycling of wastes and by-products is an effective way to deal with the economic and ecological constraints of recent decades. The valorization of industrial by-products in civil engineering is a common practice either by their incorporation during the manufacture of Portland cements or as a partial replacement of cement during the production of concrete. The present work aims to develop waste-based alkali-activated materials WAAMs intended for civil engineering applications as a potential alternative to cement-based materials. A steel industrial by-product called commonly granulated blast furnace slag GBFS was used alone as a solid CaO-rich precursor; two alkaline activators such us sodium silicate (Na_2SiO_3) and sodium hydroxide (NaOH) were used separately for the production of two-part alkali-activated materials. Besides the microstructure analysis of the hardened samples, the influence of activator/precursor mass ratio, NaOH molarity, and two curing environments (Room temperature and 60°C) on the compressive strength, water accessible porosity, mass loss, and drying shrinkage were assessed. The results showed that a high Liquid/Solid ratio leads to a decrease in the compressive strength of the samples, while high NaOH molarity significantly improves the mechanical properties by reducing the porosity of the specimens. Moreover, alkaline silicate activator provides higher compressive strengths compared to the alkaline hydroxide activator, especially when the samples were cured at room temperature where a maximum 28days-compressive strength value of 105.28 MPa was achieved. For the samples activated using sodium hydroxide solution, the results revealed that their curing at 60°C promotes obtaining high initial-compressive strengths (7 days) before decreasing subsequently as a function of the curing time. As an indication, at high alkaline concentration (NaOH = 9M), a mechanical strength decline of 21% was recorded between a curing time of 7 to 28 days. Moreover, curing at 60°C induced high porosity, significant mass loss and high drying shrinkage. SEM analysis highlighted a dense, homogeneous microstructure without apparent defects, in particular for the samples where the alkali silicate activator was used.

Keywords*: Valorization; By-product; Alkali-activated materials; Activators; Curing environment*

INTRODUCTION

Portland cement (PC), a basic constituent of mortar and concrete mixtures, is a hydraulic binder widely used in the field of civil engineering. Annually, the cement industries produce nearly 3.6 billion tons of cement and emit approximately 3.24 billion tons of CO_2 into the

atmosphere, which constitutes 5 to 7% of total greenhouse gas emissions in the world [1]. Moreover, the production of this binder requires an energy-intensive process, consuming around 20% of the industrial-energy used in Europe [2]. In order to reduce the environmental negative effect generated by the cement manufacture, particular attention is being paid to the development of new alternative eco-friendly binders. In this context, alkali-activated materials (AAMs) are being widely studied around the world to partially or totally replace PC-based systems and thus reduce global CO_2 emissions. AAMs are obtained by mixing alumino-silicate precursors and an alkaline activator, e.g., sodium hydroxide, potassium hydroxide, and sodium silicate [3, 4]. Eco-AAMs have been produced using industrial by-products (wastes) such as red mud (RM), fly ash (FA) and ground granulated blast-furnace slag (GGBFS) [5]. In addition to the reduction of carbon footprint (low CO_2 emissions) associated with their manufacture [6], these eco-materials often exhibit good properties, such as high compressive strength, low drying shrinkage, and heat resistance [7]. From three (3) industrial co-products, namely blast furnace slag, red mud and calcium carbide residue, sustainable tri-waste geopolymers were developed [8]. The result of this study showed that a maximum compressive strength of 20.3 MPa was reached at 28 days of curing recorded on the mixture containing 30% red mud (RM).

These materials which are synthesized by alkaline activation of a source of aluminosilicates are divided into two classes depending on the precursor calcium (Ca) content. In the presence of calcium ‘’Ca’’, alkaline activation (e.g. fly ash or blast furnace slag) leads to the formation of cementitious phases combined with N-A-S-H gels depending on the synthesis conditions [9]. On the other hand, systems without calcium form a three-dimensional, amorphous and totally polymerized network whose archetype is the geopolymer obtained by alkaline activation of metakaolin for example [10].

Hybrid one-part alkali-activated materials H-AAMs have been developed, mixtures composed essentially of Portland cement and industrial by-products and other natural mineral raw materials such as slag, metakaolin, fly ash, bentonite [11, 12]. In this category of hybrid materials, Abdollahnejad et al., [11] have developed mortars with 40% by weight of cement, kaolin, fly ash and calcium hydroxide being the other binding components. The air-cured specimens showed no signs of efflorescence and compressive strengths of 20 to 40 MPa were recorded at 28 days of curing. Other investigations [7, 13, 14] has focused on the development of one-part AAMs without Portland cement using co-products as basic raw materials (precursors). Sturm et al., [15] used rice husk ash as precursor and obtained 3days-compressive strength of 33 MPa.

Physical, mechanical and durability properties of blast furnace slag-based alkali-activated materials are dependent on several parameters such as activator type, its concentration in alkaline oxide (M_2O%), SiO_2/M_2O ratio where M represents the alkaline ion (e.g Na^+ or K^+) as well as the liquid/solid ratio [16, 17]. The main hydration products of alkali-activated materials whose CaO-rich precursor is used are hydrated calcium (alumino)silicates C-(A)-S-H with a tobermorite-type model structure as well as the formation of hydrotalcite, two minerals which confer the resulting material good mechanical properties [18, 19].

Curing regimes of alkali-activated materials represent another major factor that significantly influences the properties of AAMs [20]. Generally, geopolymers and AAMs are cured either at ambient temperature (around 25°C) or slightly higher temperatures (40-80°C) depending on the precursors used, mix design, etc. Suwan and Fan [21], pointed out that the heat generated following the dissolution of solid activators in one-part geopolymers could have a beneficial effect on the hardening of the specimens. Peng et al., [22], obtained a significantly low 28-day

compressive strength (< 5 MPa) for samples based on a bentonite/dolomite mixture cured for three (3) days at 20°C. On the other hand, at 80°C, the compressive strength reached 38.3 MPa. Generally, heat curing accelerates early strength development of geopolymers [23, 24]. Besides temperature, relative humidity RH is another important parameter to control during curing. It is generally preferable to seal the geopolymer because dehydration leads to efflorescence, microcracking and a significant decrease in compressive strength [25]. According to Van Deventer et al., [23], optimum curing occurs under saturated conditions (i.e. 100% relative humidity) and there is no need to add water during curing. In addition to CO_2 curing [26], geopolymers have also been cured in water tanks [14].

Granulated blast furnace slag-based alkali-activated materials are considered as potential alternatives to cement-based binders. Slags can show wide variations in their chemical and physical properties since they are industrial by-products resulting from ore of often variable chemical and mineralogical compositions. Moreover, their glassy content, which depends on the rate and type of cooling regime, can significantly affect their potential for the production of AAMs.

When GGBFS alone is used as precursor material, the results showed that higher compressive strength is obtained compared to samples having both GGBFS and fly ash as precursor materials [27]. In addition, the slag composition and its reactivity influenced the reaction kinetics of these materials and can develop widely varying mechanical strengths despite their activation by the same type of alkaline activator [28].

Blast furnace slag is often combined with other co-products (waste) for the manufacture of alkali-activated materials, such as fly ash [27], washing aggregate sludge [29]; boron waste [30]; sludge waste [31, 32]. Slags of specific compositions (Fe-rich fayalite slag (FS), ferronickel slag (FNS)) have also been the subject of investigations with the aim of developing alkali-activated materials [33, 34]. The effects of ion species and alkalinity are studied; the results showed that more C-A-S-H gels were produced than the crystalline phases at lower activator concentration, while more crystalline phases formed at high concentration [34].

Drying shrinkage evaluation of a one-part alkali-activated slag concrete for up to 180 days as a function of mix design parameters has been investigated [35]. The mix design parameters were alkaline activator to slag ratio, water to binder ratio, silica fume to binder ratio, and two curing regimes, in water and sealed plastic bag. The results showed nearly 75% of the 180-day shrinkage was reached within 20 days. Moreover, the correlation between the drying shrinkage and microscopic characteristics of the alkali-activated pastes is also investigated. Indeed, by affecting the reaction degree of the pastes, the alkali content and activator modulus cause different pore-size distributions and deformation abilities, leading to different capillary pressures and shrinkage of the pastes during drying [36]. Furthermore, drying shrinkage model for alkali-activated slag concrete was developed by Ou et al., [37].

Due to the large global demand for materials, especially those with low environmental impact, recovery and reuse of industrial by-products (waste) are highly encouraged. Granulated blast furnace slag (GBFS) is a co-product of the manufacture of cast iron and steels in blast furnaces, in addition to calcium oxide; it also contains silicates and aluminates with variable contents depending on the composition of the raw material (iron ore) as well as the technological process followed. Due to its calcium oxide content, which is often high, this industrial waste is considered as CaO-rich precursor in the manufacture of alkali-activated materials AAMs.

In Algeria, GBFS is produced exclusively by El Hadjar steel plant, located in the east of the country. This industrial by-product, generated in considerable quantities, is often used as a

cementitious additive during the manufacture of compound cements and concrete production. Besides the economic and environmental benefits, the use of the Algerian GBFS has improved many technological properties of cementitious materials. On the other hand, this local waste is rarely used as a precursor for the production of alkali-activated materials or geopolymers. This present experimental work focused on the possibility of using this local industrial co-product alone as a basic raw material (precursor) for the development of alkali-activated materials as a case study which falls within the framework of the recovery of industrial wastes and the production of eco-materials. The main purpose of this investigation is to study the impact of mix design parameters including the alkaline activator type (Na_2SiO_3 and NaOH), NaOH molarity, the liquid to solid ratio, and two curing environments on the compressive strength, water accessible porosity, drying shrinkage, and the microstructure of the GBFS-alkali-activated materials developed.

MATERIALS AND METHODS

Raw materials

Calcium-rich precursor was used as a basic raw material to produce alkali-activated materials (AAMs). It is a by-product of the steel industry, commonly called granulated blast-furnace slag GBFS. This industrial co-product was recovered from *El Hadjar* steel plant (Annaba-Algeria). First, this waste-material was dried, crushed before being finely ground. Its Blaine specific surface after grinding is evaluated at 6789 cm^2/g. The chemical composition in oxides of the GGBFS carried out through X-ray fluorescence is displayed in Table 1. With a content of 40.35%, this slag is considered a CaO-rich precursor.

***Table 1**. Chemical composition of GGBFS*

Oxide	Na_2O	MgO	Al_2O_3	SiO_2	P_2O_5	SO_3	K_2O	CaO	TiO_2	MnO	Cr_2O_3
Content (%)	0.32	3.00	7.46	39.88	0.01	1.19	0.92	40.35	0.30	2.40	1.95
Oxide	Fe_2O_3	V_2O_5	NiO	CuO	ZnO	SrO	Rb_2O	PbO	ZrO_2	BaO	LOI
Content (%)	0.001	0.001	0.0022	0.0041	0.0024	0.210	0.0027	0.001	0.03	2.09	0.00

Crystallinity and slag phases were analyzed by XRD as shown in Figure 1. The result revealed, in addition to the amorphous character, the presence of crystalline phases composed essentially of quartz in addition to carbonates (calcite and dolomite). Peaks of pyrite were also detected.

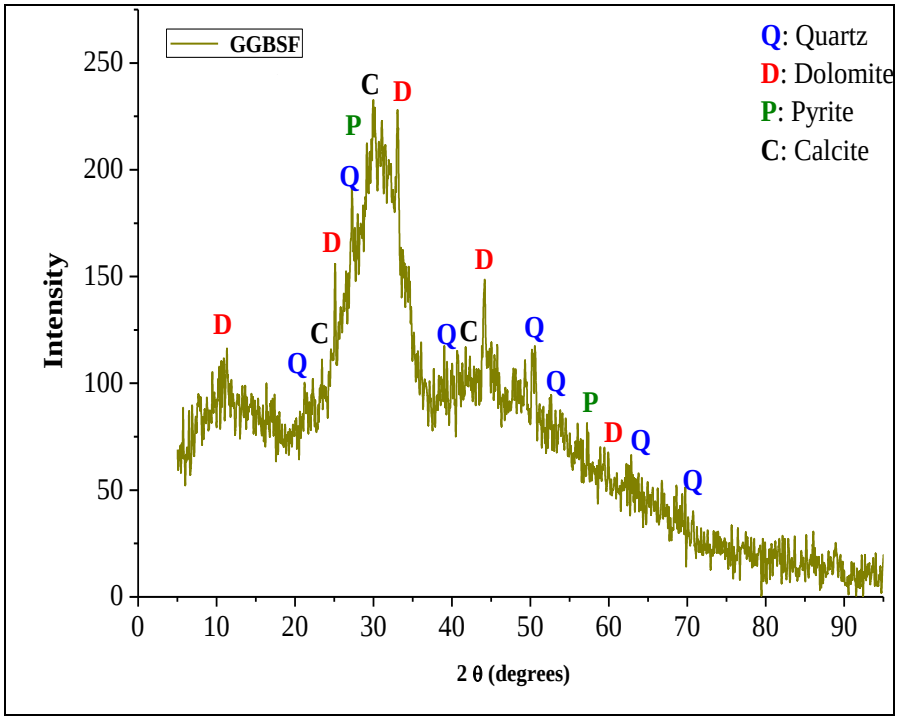


Fig. 1. XRD pattern of the GGBFS

The Particle size distribution of the ground granulated blast furnace slag (GGBFS) used in this experimental study is showed in Figure 2. This analysis was performed using LA-950 particle size analyzer.

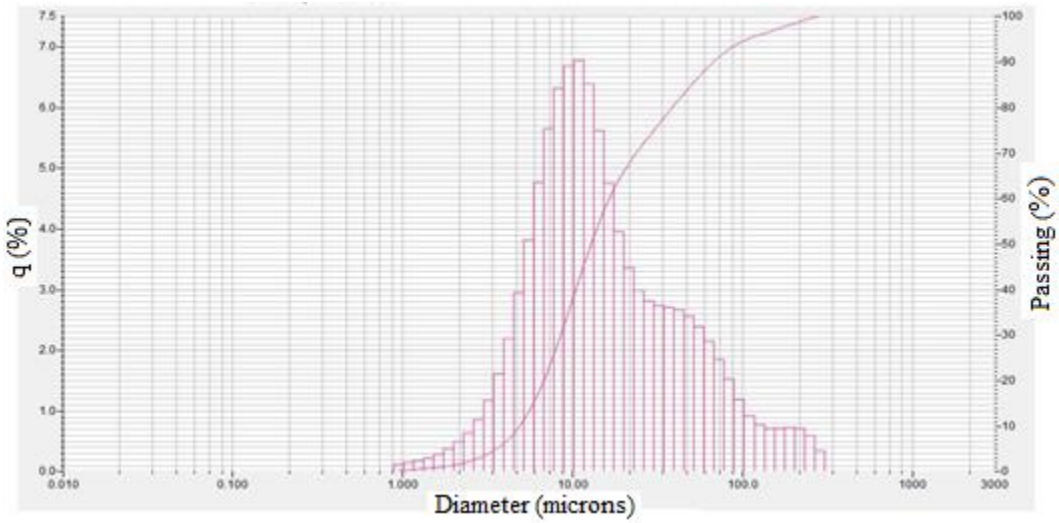


Fig. 2. Particle size distribution of the ground slag powder

Particle size analysis revealed the presence of a population of particles varying between 1.31 µm and 262.37 µm with a median size of 14.36 µm.

The liquid alkaline activators used in this investigation were sodium hydroxide solutions of different concentrations (5M; 7M and 9M), obtained by dissolving alkali hydroxide pellets (NaOH, purity 96%) in distilled water, and sodium silicate solution Na_2SiO_3 having the following characteristics: Na_2O=14.50%, SiO_3=30.7%, $SiO_3/Na_2O \approx 2.07$ and 44.57% of dry matter.

Sample preparation and curing conditions

The first series of alkali-activated material samples was prepared by mixing sodium hydroxide solution of known molar concentration (5M, 7M or 9M) with ground blast furnace slag powder according to a liquid/solid (L/S) mass ratio equal to 0.3. This ratio of 0.3 was set after carrying out preliminary optimization tests, i.e. obtaining a homogeneous paste of optimal consistency. A second series of AAM samples was prepared using sodium silicate solution (Na_2SiO_3) as activator. Liquid/solid mass ratios of 0.42; 0.47 and 0.52 (Activator/Precursor) have been applied (tested). These ratios correspond respectively to alkaline silicate contents of 6.09%, 6.81% and 7.54% (expressed as Na_2O% relative to the mass of precursor).

The mixtures are thoroughly homogenized using a *Controlab* brand mixer in accordance with standard NF EN 196-3 [38]. The pastes obtained were immediately molded in prismatic molds of 40×40×160 mm^3 as shown in Figure 3. After 24 hours, the AAM specimens were removed from the mold; then cured in two different environments:

– At Room temperature (Ambient laboratory conditions T = 24±1 °C);

– At 60 °C (in an oven).

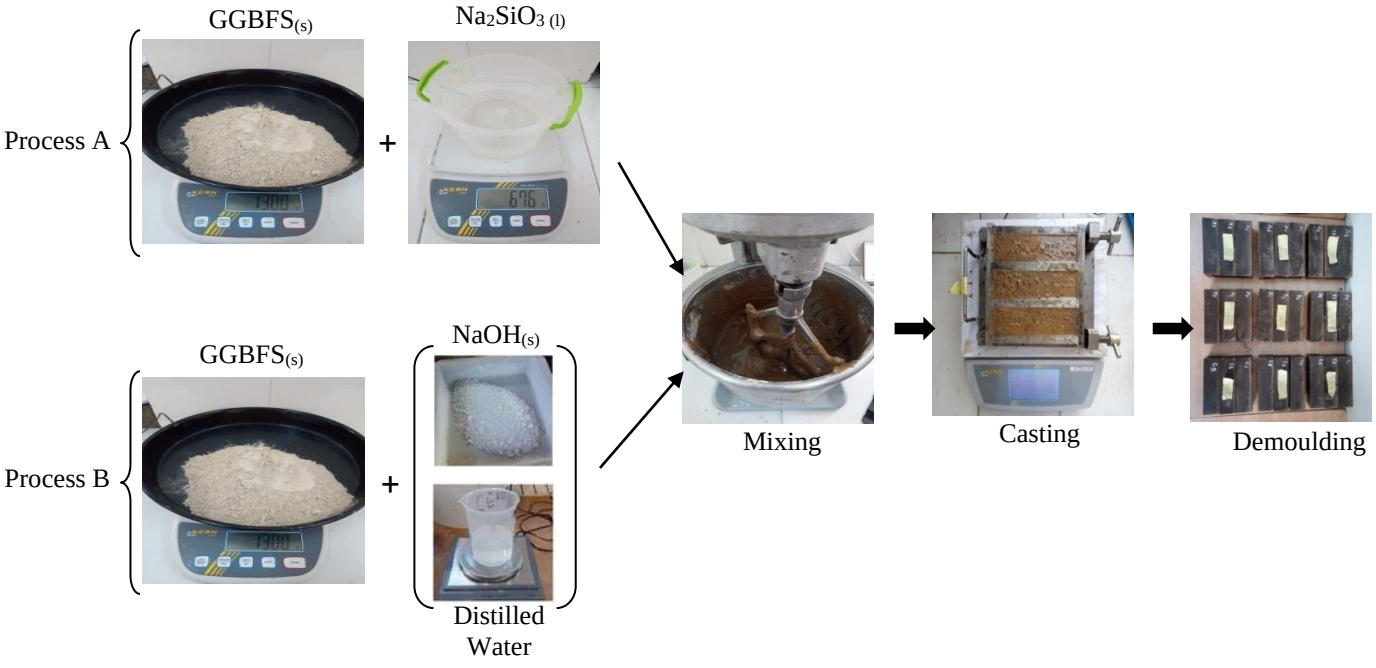


Fig. 3. Manufacturing processes used for the preparation of alkali-activated pastes

Codes are assigned to the different mixtures according to:

a) Material:
- AAM: Alkali-activated material

b) Type of the activator used:
- AS: Alkaline silicate (Na_2SiO_3);
- AH: Alkali hydroxide (NaOH)

c) Activator content:
- 0.42; 0.47; 0.52: Activator/Precursor mass ratios;
- 5M; 7M; 9M: Molar concentrations of sodium hydroxide solution

d) Curing environment:
- T60: Cured at 60 °C;
- RT: Cured at room temperature

For example: AAM-AS-0.42-RT: Alkali-Activated Material dosed using Alkaline Silicate activator with an activator/precursor mass ratio = 0.42, cured at Room Temperature.

Characterization tests

The hardened alkali-activated materials have undergone various characterization tests. Compressive strength of the specimens was performed in accordance with standard NF EN 1015-11 [39], using a Cyber-Tronic electo-hydraulic testing press, where the breaking stress is recorded. This mechanical test was carried out at 2, 7 and 28 days of curing. Three iterations were conducted for each sample series, the average value of these iterations is taken as the compressive strength of the sample. Water accessible porosity was determined using dry and saturated mass variation method. First, a saturated sample was surface dried and then its mass was evaluated. The sample is then dried at 105 °C until obtaining constant mass, after which its dry mass is measured. The porosity was calculated from the variation of the dry and saturated masses of the specimen, the value is expressed as a percentage. Porosity test was carried out according to standard NF P18-459 [40]. The porosity (Po) is calculated according to the formula (1)

$$\mathrm{Po} = \frac{\mathrm{Ms}-\mathrm{Md}}{V} 100\% \quad (1)$$

Ms: Mass of the saturated specimen;
Md: Mass of the dry specimen;
V: Volume of the specimen.

Drying shrinkage represents volumetric changes. In our practical case, drying shrinkage was measured using a caliper at 28 days of curing. The drying shrinkage measured takes into consideration the average of the longitudinal and transverse dimensional variations with respect to the initial dimensions of the specimen. The mass loss was evaluated using an analytical balance. It represents the sample difference mass, weighed just after demoulding (1 day) and at 28 days. Scanning electron microscopy (SEM) analysis was realized to highlight the morphology and microstructure of the hardened samples using *Philips ESEM XL30* scanning electron microscope.

RESULTS AND DISCUSSION

Compressive strength

Depending on the curing environment and the alkaline silicate content of the activator, Figures 4 and 5 show the evolution of the compressive strength of the AAM specimens as a function of the curing time.

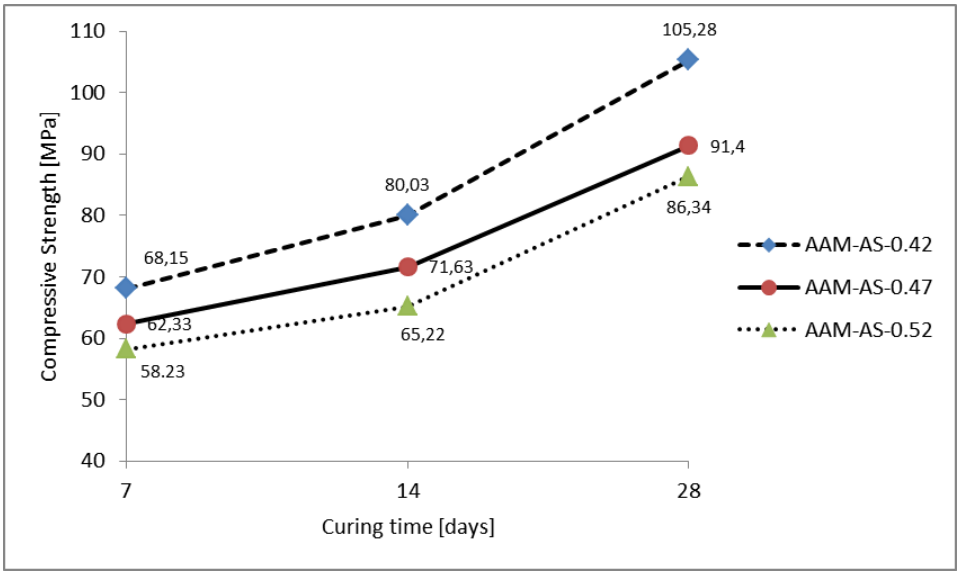


Fig. 4. Compressive strength evolution of the materials activated using sodium silicate solution, cured at room temperature

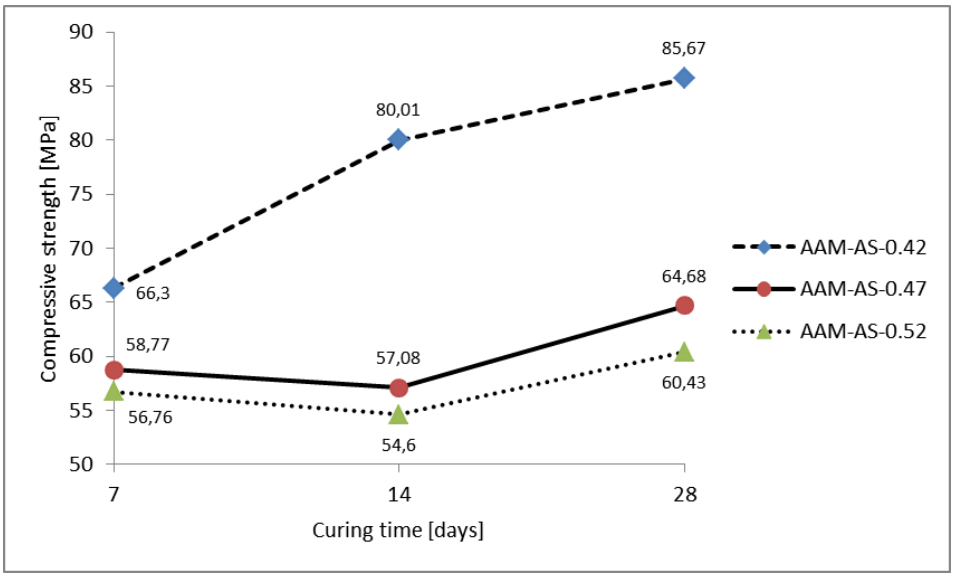


Fig. 5. Compressive strength evolution of the materials activated using sodium silicate solution, cured at 60°C

According to the results illustrated in Figure 4, we can notice that the compressive strength of the samples increases significantly as a function of the curing time (from 7 to 28 days) and

this, for the three series of samples. However, lower compressive strength values were obtained when a high liquid/solid (activator/precursor) mass ratio was used, this can be explained by the large amount of liquid (water contained in the activator solution) which subsequently results in material with high porosity. The highest compressive strength value (105.28 MPa) was recorded at 28 days of curing at room temperature and a lowest liquid to solid ratio equal to 0.42, the latter corresponding to an alkaline silicate content of 6.09% (expressed as Na_2O% relative to the precursor mass).

For samples cured at 60°C (Figure 5), the improvement in compressive strength as a function of curing time is not so significant compared to samples cured at room temperature. As an indication, for sample AAM-AS-0.42, a compressive strength value of 66.3 MPa was recorded at 7 days of curing at 60°C before reaching 85.67 MPa at 28 days; which represents a strength gain of 29.21%. However, for the same variety of sample (AAM-AS-0.42) cured at room temperature, respective strength values of 68.15 MPa and 105.28 MPa were recorded at 7 days and 28 days of curing; which corresponds to a gain resistance of 54.48%. For the other two series of samples (AAM-AS-0.47 and AAM-AS-0.52), respective mechanical strength gains of 46.63% and 48.27% were calculated for the samples cured at room temperature against only 10.05% and 6.46 % for specimens cured at 60°C.

Overall, the use of alkaline silicate solution as an activator gave excellent mechanical performance with extremely high compressive strength values. This can be explained by the fact that alkaline silicates, due to their high pH, attack the vitreous network of the slag and promote the dissolution and precipitation of hydrotalcite and C-A-S-H. Alkaline silicates are particularly effective (generally more than hydroxides) because they already contain silica in solution, which makes it easier to initiate the formation of reaction products and therefore the rapid development of resistances, so well that it is possible to achieve very high initial strengths [41].

The results of the compressive strength of the AAMs when alkali hydroxide activator is used (sodium hydroxide solution) are given respectively in Figures 6 and 7. The curing of the specimens was carried out in two different environments: at room temperature and at 60°C.

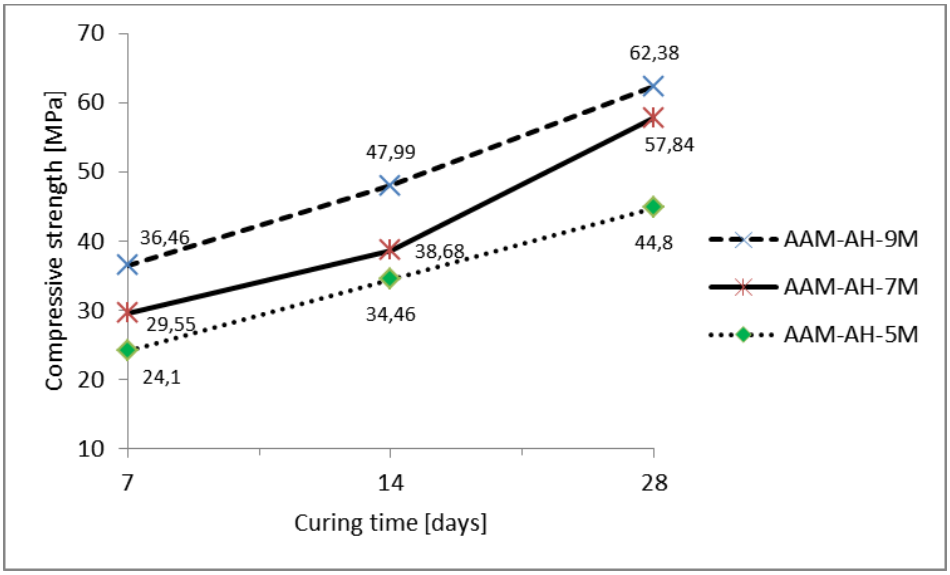


Fig. 6. Evolution of the compressive strength of the materials activated using sodium hydroxide solution (NaOH) at different molar concentrations; cured at room temperature

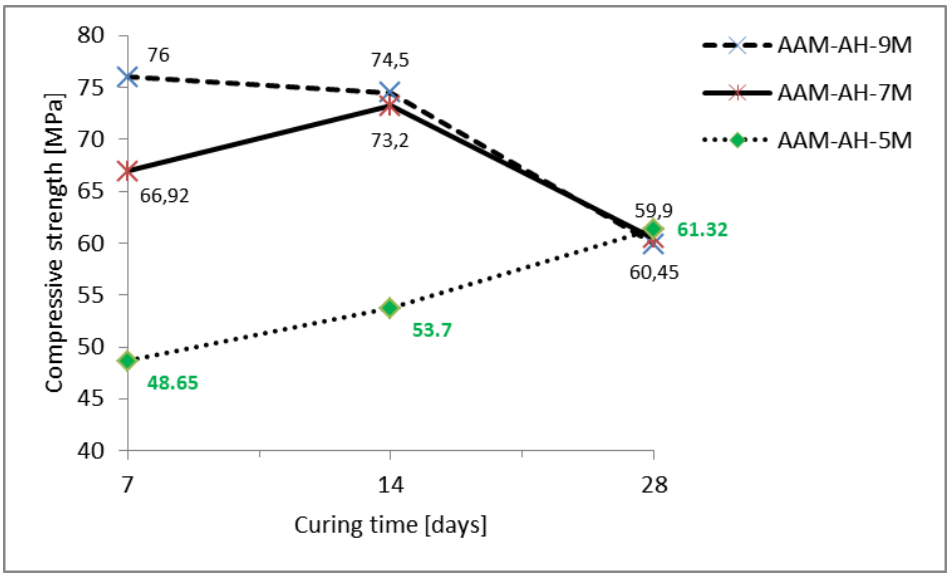


Fig. 7. Evolution of the compressive strength of materials activated using sodium hydroxide solution (NaOH) at different molar concentrations, cured at 60°C

According to the results highlighted in Figure 6, it can be observed that the compressive strength of all the AAMs improves with the increase in activator concentration (sodium hydroxide solution). It can be noticed that the sample activated using a low concentrated solution (AAM-AH-5M) has a compressive strength of 44.8 MPa at 28 days, when the concentration of the activator increases to 7M (AAM-AH -7M), the compressive strength of the specimen enhances to 57.84 MPa before reaching a maximum value of 62.38 MPa at 28 days of curing at room temperature when the concentration of the activating solution is equal to 9M. Overall, it can be concluded that the compressive strength of samples activated using an alkali hydroxide based activator (NaOH) increases significantly with increasing concentration hydroxide ions OH^- in the alkaline solution.

Moreover, the increase in the NaOH molarity favors the dissolution of the binder and the formation of more hydration products (C-S-H and C-A-S-H) thus improving the mechanical resistance of the material [42].

It can also be deduced that the curing time at ambient environment has a positive influence on the evolution of the compressive strength of the AAMs. As an indication, for the AAM-AH-9M sample, a value of 36.46 MPa was recorded at 7 days of curing, it reached 47.99 MPa at 14 days and 62.38 MPa at 28 days. This enhancement in the mechanical resistance can be explained by the development of hydration reactions and the formation of calcium hydrosilicates C-S-H and C-A-S-H responsible for the improvement of mechanical performance [43].

The results in Figure 7 clearly show that curing the AAM-AH samples at temperature of 60 °C promotes obtaining high initial compressive strength values. The values recorded at 7 days represent at least the double of the values obtained at room temperature curing. For example, disparate values of 76 MPa and 36.46 MPa were obtained after 7 days for the AAM-AH-9M sample cured at 60 °C and room temperature respectively. This phenomenon is possibly due to the acceleration of the hydration process and the rapid formation of hydrates under the effect of heat. We can also notice the reduction in mechanical resistance as a function of curing time,

especially for samples where the concentration of the activator is high (7M and 9M). Finally, it is useful to point out the convergence of all the resistances to a value of around ≈ 60 MPa after 28 days of hardening, thus becoming almost equivalent to those recorded for the samples cured at room temperature. According to the study conducted by Fernández-Jiménez et al., [44], a fairly high curing temperature (60 °C) has different effects depending on the category (type) of the activator used. The mechanical resistances can be slowed down and give less interesting values with certain activators when the temperature is high. The explanation of this phenomenon is based on the fact of the formation of a large amount of hydration products at a young age, which leads to a consequent densification of the matrix and a modification of the microstructure. Therefore, over time, diffusion processes are more difficult and reactions are decelerated.

Water accessible porosity

Figure 8 illustrates the evolution of the porosity accessible to water of the materials activated using sodium silicate solution as a function of the mass ratio (activator/precursor). The porosity tests were carried out at 28 days of curing on samples kept in two different environments.

The results show that a high liquid/solid ratio (activator/precursor) leads to an increase in the samples porosity; this is valid for the two sample storage environments. On the other hand, this increase in porosity is more significant and quasi-linear with greater slope when the samples were cured at temperature of 60°C. This increase in porosity especially under temperature of 60°C can be attributed to the amount of water that evaporates leaving voids after evaporation; the latter which accelerates and intensifies under the effect of heat. Values of 6.76% and 8.67% were measured at 28 days in the two respective storage environments (at room temperature and at 60°C).

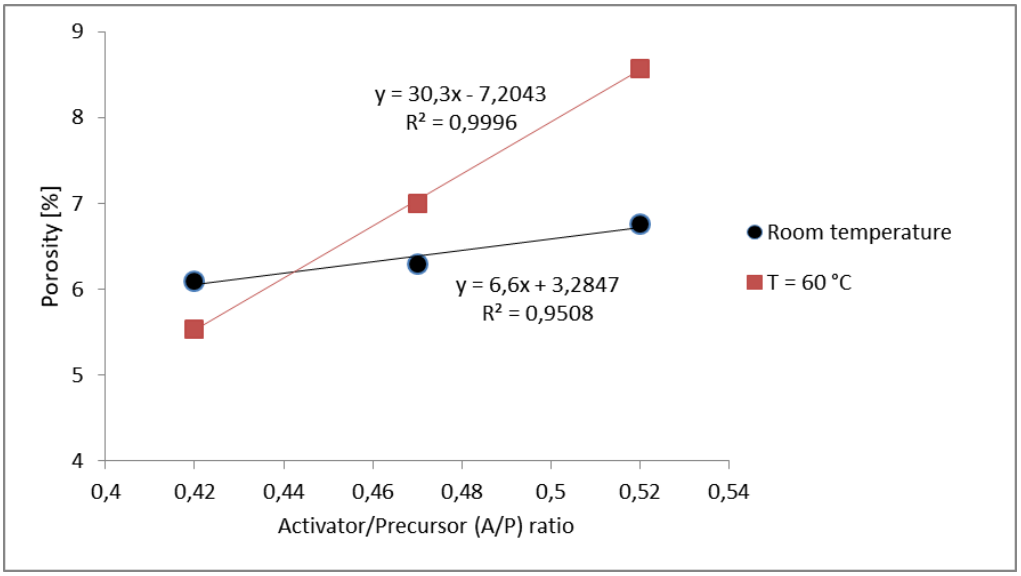


Fig. 8. Evolution of the porosity of AAMs according to the Activator/Precursor ratio and the storage conditions of the samples

Figure 9 shows the evolution of the porosity of alkali-activated materials as a function of the concentration of sodium hydroxide solution (activator). It should be noted that the activator to precursor mass ratio was set at 0.3. The results in Figure 9 indicate that the use of sodium hydroxide solution as an activator gives high porosities compared to samples activated using sodium silicate solution. Indeed, with a concentration of 5M, respective values of 19.9% and 14% were measured depending on the curing conditions. However, the use of a high concentration activator (NaOH = 9M) effectively contributes to reducing the porosity of the samples. A minimum value of 3.7% was measured with a concentration of 9M for a sample cured at room temperature.

Indeed, a high NaOH molarity gave rise to a lower porosity, this is due to the fact that the solution contains more solute (NaOH pellets) for the same volume of solvent (distilled water), and thus the solution becomes more viscous, which reduces water evaporation during the curing process. Furthermore, increasing the molarity of the NaOH solution favors the dissolution of the binder and the formation of more hydration products [42].

Furthermore, the porosities values recorded seem well correlated with the compressive strength results, i.e, a high porosity disadvantages the development of mechanical resistance.

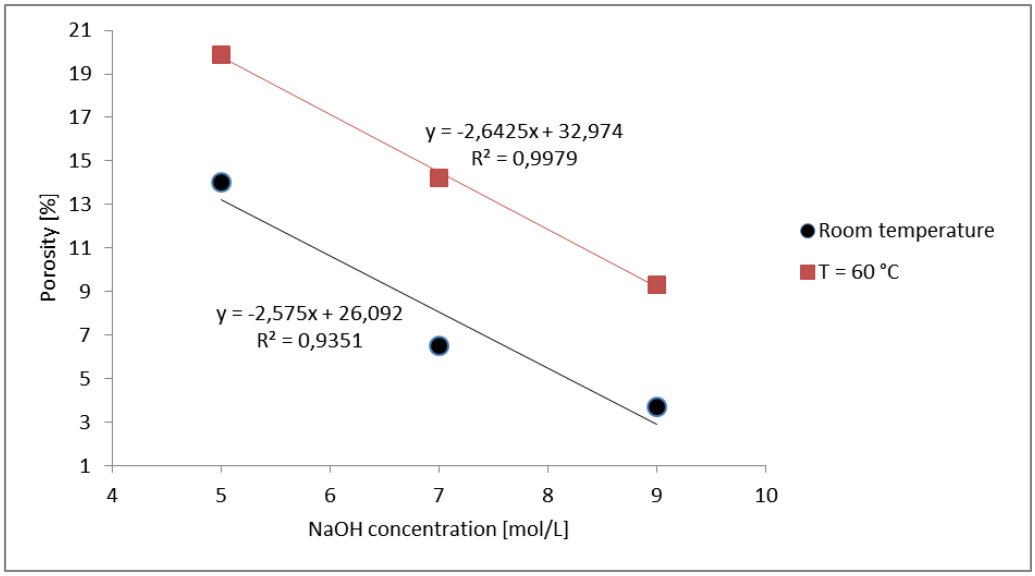


Fig. 9. Evolution of the porosity of AAMs as a function of the concentration of the sodium hydroxide solution

Mass loss and drying shrinkage

Figures 10 and 11 respectively illustrate mass loss and drying shrinkage of the alkali-activated materials (AAMs) produced according to the activator type used, its concentration as well as the curing conditions of the samples.

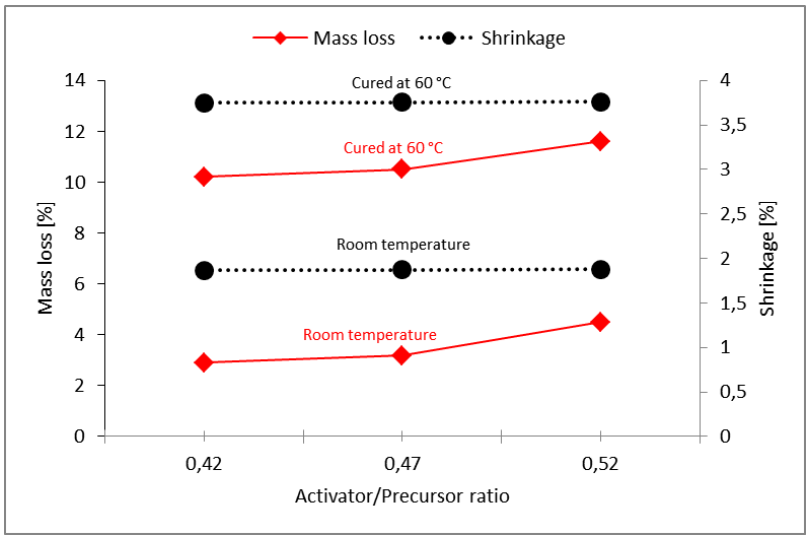


Fig. 10. Mass loss and drying shrinkage of samples activated using sodium silicate solution Na2SiO3

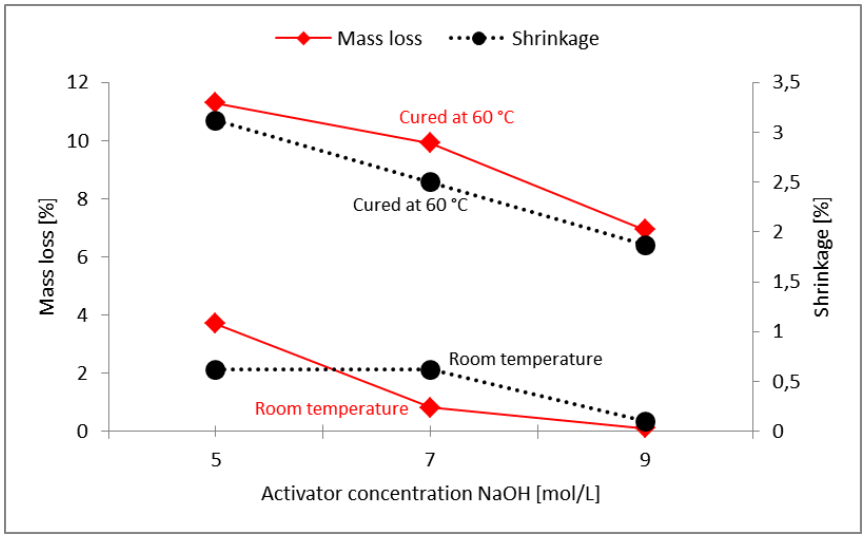


Fig. 11. Mass loss and drying shrinkage of samples activated using sodium hydroxide solution NaOH

From Figure 10, it can be seen that samples cured at 60 °C experienced greater mass loss and drying shrinkage compared to samples cured at room temperature. Respective maximum rates of 11.6% and 3.76% were recorded with an Activator/Precursor ratio equal to 0.52. The results also report a slight mass loss of AAM-AS (about ≈1.5%) depending on the evolution of the Activator/Precursor mass ratio. On the other hand, drying shrinkage remains stable despite a higher Activator/Precursor ratio for both curing environments. This phenomenon is possibly due to the creation of an internal porosity without retraction of the sample dimensions.

The results in Figure 11 clearly revealed that samples-curing at high temperature (60 °C) leads to greater mass loss and drying shrinkage. In addition, the results obtained show that the activator concentration significantly influences these two properties (mass loss and drying shrinkage). However, the mass loss and drying shrinkage decrease markedly with a high concentration of the activator. Indeed, at room temperature, using a 7M sodium hydroxide

solution, respective low percentages of 0.87% and 0.62% were obtained for mass loss and shrinkage. At 9M, mass loss and sample drying shrinkage become extremely low (negligible). This effect of the activator concentration can be attributed to the fact that a solution having a high concentration contains a significant amount of solid matter (solute) and less water thus becoming more viscous, therefore, the evaporation of water and the reduction in the dimensions of the samples will be less important.

At 60°C, the rates recorded (mass loss and shrinkage) are slightly high but they remain overall lower than those recorded for the samples activated with sodium silicate solution and this, for the two curing environments studied. Moreover, varying the concentration of the activator from 5M to 9M, led to a gain in mass loss and drying shrinkage of 38.67% and 40.06% respectively. These grades were recorded for the AAM-AH samples cured at 60°C.

Microstructural analysis

Figure 12 presents a scanning electron microscope SEM analysis of the different samples of AAMs produced. This microstructural analysis was conducted on four series of samples depending on the activator type and the curing environment. The samples which provided the best mechanical resistances at 28 days were selected for the SEM analysis.

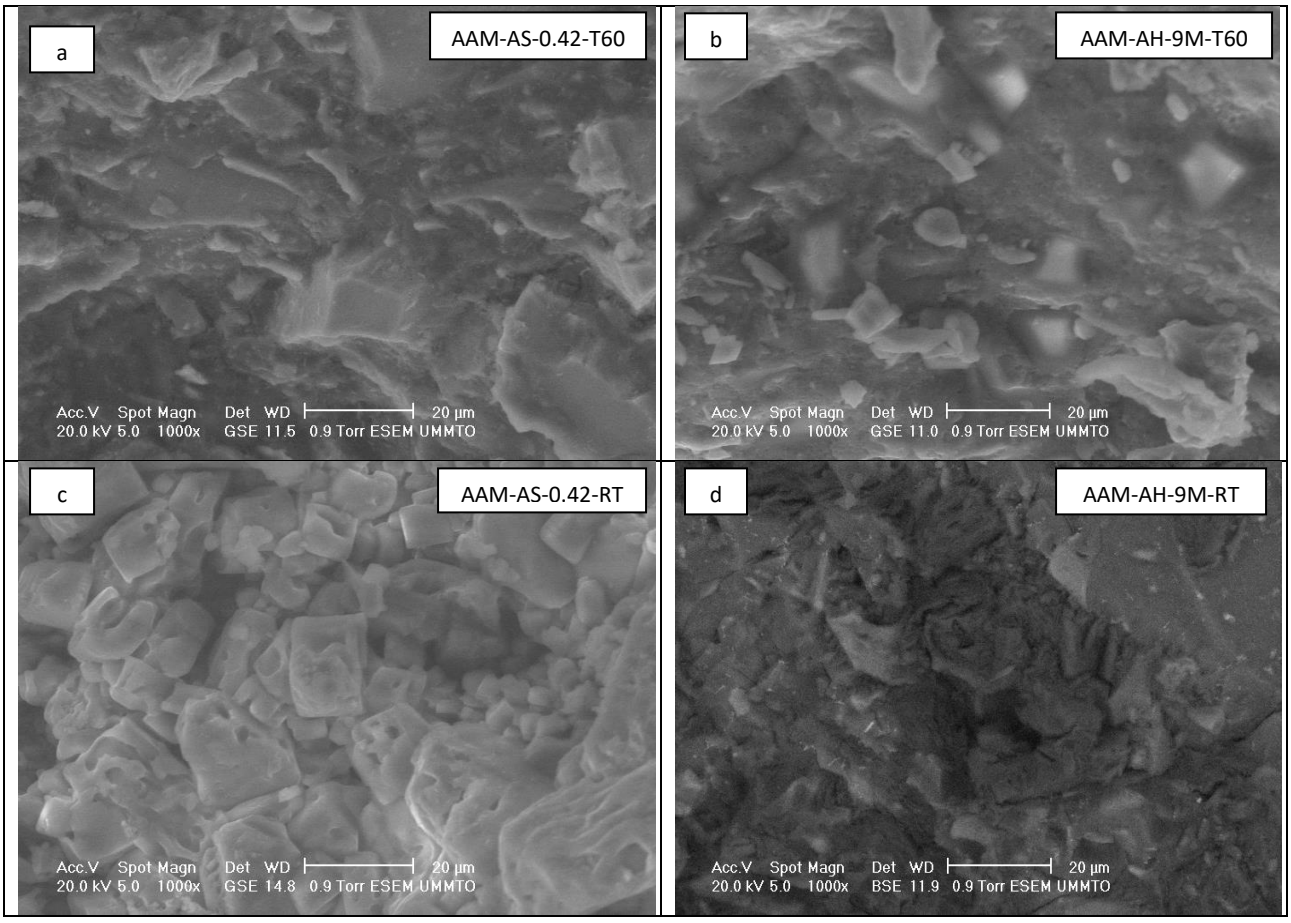


Fig. 12. SEM micrographs of the alkali-activated materials produced, depending on curing conditions and the activator type used

Microstructural analysis (Figure 12) illustrates that samples activated using the alkaline silicate solution, cured either at room temperature or at 60°C (AAM-AS-RT and AAM-AS-T60) exhibit a dense microstructure, homogeneous and without apparent defects (Figure 12(a)(b)). The AAM-AS-T60 sample reveals some unreacted GGBFS particles which would induce a reduced amount of hydration products, C-S-H and C-(N)-A-S-H gels; this is possibly due to the process of rapid hardening imposed by the high temperature (60°C).

Samples activated using NaOH alkali hydroxide solution (AAM-AH-RT and AAM-AH-T60) appear to have more porosity and less compact and less homogeneous matrices. Crystals of precise geometry are visible on samples cured at room temperature (Figure 12(c)). These crystals are not observed on the heat-cured samples (Figure 12(c)) where the usual hydration products have not had the necessary time to form, probably because of the high temperature which has disturbed their formation. SEM images (Figure 12(c)(d)) support the results of the compressive strength tests, where a significant loss of strength was recorded for samples in which alkali hydroxide (NaOH) was used as activator. The appearance of pores in these pastes may help explain the reduced strength, particularly at 28 days of curing.

Furthermore, no cracking or micro-cracks resulting from the preparation of the samples is observed on all the samples analyzed.

Overall, the SEM analysis correlates well with the results of compressive strength and water-accessible porosity.

Regarding microstructure studies, it was revealed that C-S-H and C-A-S-H gels predominate in calcium- and silicon-rich systems, whereas N-A-S-H gel forms in the absence of calcium [20, 45].

CONCLUSIONS

The present experimental research aims to valorize a CaO-rich industrial by-product, used as a precursor for the manufacture of two-part alkali-activated binders intended mainly for civil engineering applications. Based on the results obtained, the following conclusions were drawn:

- Ground Granulated Blast furnace slag GGBFS, which is an industrial co-product, can be valorized as a precursor for the manufacture of high-performance two-part alkali-activated materials. In our practical case, a maximum 28days-compressive strength of 105.28 MPa was achieved using alkaline silicate activator and Liquid/solid of 0.42.
- A high liquid to solid mass ratio promotes a drop in compressive strength and an increase in the porosity of alkali-activated materials based on blast furnace slag. Indeed, increasing the ratio from 0.42 to 0.52 causes a compressive strength decline of approximately 18% and 29%, recorded for samples cured at room temperature and at 60°C, respectively.
- High NaOH molarity significantly enhances the compressive strength, reduced samples porosity, and induced extremely low drying shrinkage.
- Curing at 60°C of GGBFS-NaOH samples promotes obtaining high initial compressive strengths (7 days) before subsequently decrease as a function of time (28 days). As an indication, at high alkaline concentration (NaOH = 9M), a mechanical strength decline of 21% was recorded between a curing time of 7 to 28 days.

- Compared to the ambient temperature, the samples-curing at 60°C induces a high porosity, a significant loss of mass and a greater drying shrinkage and consequently a drop in the mechanical resistances.
- SEM analysis highlighted a dense, homogeneous microstructure without apparent defects, in particular for the samples where the alkali silicate activator was used.
- Activated slags are different from geopolymers due to their calcium content, allowing them in particular to produce C-A-S-H. Thus, the presence of calcium makes the use of molar ratios as for activated aluminosilicates insignificant. It is entirely possible to simplify the formulation using activators as a percentage of precursors, since the slag is generally almost totally reactive. In this case, we are closer to the formulation of Portland cement.

Declarations:

Conflicts of Interest

The authors declare that they have no known financial interests or personal relationships that could have appeared to influence the work reported in this paper.

REFERENCES

1. Wang W.C., Wang H.Y., Tsai H.C.: Study on engineering properties of alkali-activated ladle furnace slag geopolymer. Construction and Building Materials 123 (2016) 800–805.
2. Gonçalves M., Vilarinho I.S., Capela M., Caetano A., Novais R.M., Labrincha J.A., Seabra M.P.: Waste-Based One-Part Alkali Activated Materials. Materials 14 (2021), 2911.
3. Omur T., Kabay N., Miyan N., Ozkan H., Ozkan C.: The effect of alkaline activators and sand ratio on the physico-mechanical properties of blast furnace slag based mortars. Journal of Building Engineering 58 (2022) 104998.
4. Davidovits J.: Geopolymer: chemistry and application. J. Davidovits [ed.], Institut Géopolymère, Saint-Quentin, France, 2008.
5. Reddy M.S., Dinakar P., Rao B.H.: Mix design development of fly ash and ground granulated blast furnace slag based geopolymer concrete. Journal of Building Engineering 20 (2018) 712–722.
6. Duxson P., Fernandez-Jimenez A., Provis J.L., Lukey G.C., Palomo A., Deventer J.: Geopolymer technology: the current state of the art. Journal of Materials Science 42 (9) (2007) 2917–2933.
7. Oderji S.Y., Chen B., Ahmad M.R., Shah S.F.A.: Fresh and hardened properties of one-part fly ash-based geopolymer binders cured at room temperature: Effect of slag and alkali activators. Journal of Cleaner Production 225 (2019) 1–10.
8. An Q., Pan H., Zhao Q., Wang D.: Strength development and microstructure of sustainable geopolymers made from alkali-activated ground granulated blast-furnace slag, calcium carbide residue, and red mud. Construction and Building Materials 356 (2022) 129279.

9. Garcia-Lodeiro I., Palomo A., Fernández-Jiménez A., Macphee D.E.: Compatibility studies between N-A-S-H and C-A-S-H gels. Study in the ternary diagram Na_2O–CaO–Al_2O_3–SiO_2–H_2O. Cement and Concrete Research 41 (2011) 923–931.
10. Davidovits J., Geopolymers inorganic polymeric new materials. Journal of Thermal Analysis and Calorimetry 37 (1991) 1633–1656.
11. Abdollahnejad Z., Pacheco-Torgal F., De Aguiar J.B.: Eco-concrete: One-part geopolymer mixes. Proce. TRF Senior Research Scholars Progress II, Khon Kaen, Thailand, 2013. pp. 1-7
12. Askarian M., Tao Z., Adam G., Samali B.: Mechanical properties of ambient cured one-part hybrid OPC-geopolymer concrete. Construction and Building Materials 186 (2018) 330–337.
13. Askarian M., Tao Z., Samali B., Adam G., Shuaibu R.: Mix composition and characterisation of one-part geopolymers with different activators. Construction and Building Materials 225 (2019) 526–537.
14. Nematollahi B., Sanjayan J., Qiu J., Yang E.: Micromechanics-based investigation of a sustainable ambient temperature cured one-part strain hardening geopolymer composite. Construction and Building Materials 131 (2017) 552‑563.
15. Sturm P., Gluth G.J.G., Brouwers H.J.H., Kühne H.C.: Synthesizing one-part geopolymers from rice husk ash. Construction and Building Materials 124 (2016**)** 961–966.
16. Karam R., Paris M., Deneele D., Wattez T., Cyr M., Bulteel D.: Effect of sediment incorporation on the reactivity of alkali-activated GGBFS systems. Materials and Structure (2021) 54 118.
17. Marvila M.T, De Azevedo A.R.G, Oliveira L.B, Xavier G.D.C, Fontes Vieira C.M. : Mechanical, physical and durability properties of activated alkali cement based on blast furnace slag as a function of %Na_2O. Case Studies in Construction Materials 15 (2021) e00723.
18. Provis J.L., Bernal S.A.: Geopolymers and Related Alkali-Activated Materials. Annual Review of Materials Research 44 (2014) 299–327.
19. Provis J.L., Van Deventer J.S.J., Alkali Activated Materials. State-of-the-Art-Report, J.L. Provis and J.S.J. Van Deventer [eds.], New York London, 2014.
20. Guo W., Zhao Q., Sun Y., Xue C., Bai Y., Shi Y.: Effects of various curing methods on the compressive strength and microstructure of blast furnace slag-fly ash-based cementitious material activated by alkaline solid wastes. Construction and Building Materials 357 (2022) 129397.
21. Suwan T., Fan M.: Effect of manufacturing process on the mechanisms and mechanical properties of fly ash-based geopolymer in ambient curing temperature. Materials and Manufacturing Processes 32 (2017) 461‑467.
22. Peng M.X., Wang Z.H., Xiao Q.G., Song F., Xie W., Yu L.C., Huang H.W., Yi S.J.: Effects of alkali on one-part alkali-activated cement synthesized by calcining bentonite with dolomite and Na_2CO_3. Applied Clay Science 139 (2017) 64‑71.
23. Van Deventer J.S.J., Feng D., Duxson P.: Dry mix cement composition, methods and system involving same. Patent N° 7,691,198 B2, USA, 2010.
24. Li X., Wang Z., Jiao Z.: Influence of curing on the strength development of calcium-containing geopolymer mortar. Materials 6 (2013) 5069‑5076.
25. O'Connor S.J., MacKenzie K.J.D.: Synthesis, characterization and thermal behavior of lithium aluminosilicate inorganic polymers. Journal of Materials Science 45 (2010) 3707‑3713.

26. Jun Y., Han S.H., Kim J.H.: Early-age strength of CO_2 cured alkali-activated blast furnace slag pastes. Construction and Building Materials 288 (2021) 123075.
27. Manojsuburam E., Sakthivel E., Jayanthimani E.: A study on the mechanical properties of alkali activated ground granulated blast furnace slag and fly ash concrete, Materials Today: Proceedings 62 (2022) 1761–1764.
28. Marsh A.T.M., Yue Z., Dhandapani Y., Button K., Adu-Amankwah S., Bernal S.A.: Influence of limestone addition on sodium sulphate activated blast furnace slag cements. Construction and Building Materials 360 (2022) 129527.
29. Bilici S., Kabay N., Miyan N., Omur T., Ozkan H.: Effect of washing aggregate sludge waste on the properties of alkali-activated blast furnace slag. Journal of Building Engineering 63 (2023) 105527.
30. Yon MS., Karatas M.: Evaluation of the mechanical properties and durability of self-compacting alkali-activated mortar made from boron waste and granulated blast furnace slag. Journal of Building Engineering 61 (2022) 105263.
31. Duan W., Zhuge Y, Chow W.K.C, Keegan A., Liu Y., Siddique R.: Mechanical performance and phase analysis of an eco-friendly alkali-activated binder made with sludge waste and blast-furnace slag. Journal of Cleaner Production 374 (2022) 134024.
32. Wang Q., Sun S., Yao G., Wang Z., Lyu X.: Preparation and characterization of an alkali-activated cementitious material with blast-furnace slag, soda sludge, and industrial gypsum. Construction and Building Materials 340 (2022) 127735.
33. Adediran A., Yliniemi J., Lemougna P.N., Perumal P., Illikainen M.: Recycling high volume Fe-rich fayalite slag in blended alkali-activated materials: Effect of ladle and blast furnace slags on the fresh and hardened state properties. Journal of Building Engineering 63 (2023) 105436.
34. Huang Z., Wang Q., Lu J.: The effects of cations and concentration on reaction mechanism of alkali-activated blast furnace ferronickel slag. Composites Part B 236 (2022) 109825.
35. Sadeghian G., Behfarnia K., Teymouri M.: Drying shrinkage of one-part alkali-activated slag concrete. Journal of Building Engineering 51 (2022) 104263.
36. Huang D., Yuan Q., Chen P., Tian X., Peng H.: Effect of activator properties on drying shrinkage of alkali-activated fly ash and slag. Journal of Building Engineering 62 (2022) 105341.
37. Ou Z., Feng R., Li F., Liu G., Li N.: Development of drying shrinkage model for alkali-activated slag concrete. Construction and Building Materials 323 (2022) 126556.
38. NF EN-196-3: Méthodes d'essai des ciments - Partie 3: Détermination du temps de prise et de la stabilité, septembre 2017.
39. NF EN1015-11: Méthodes d'essai des mortiers pour maçonnerie - Partie 11: Détermination de la résistance en flexion et en compression du mortier durci. Novembre 2019.
40. NF P18-459 : Béton - Essai pour béton durci - Essai de porosité et de masse volumique.
41. Oualit M., Irekti A., Sarri A. Influence des conditions de durcissement et le taux d'alcalins sur les performances mécaniques des matériaux alcali-activés à base du laitier de haut fourneau. Matériaux & Techniques 110 (2022) 202.
42. Gijbelsa K., Pontikesb Y., Samync P., Schreursa S., Schroeyersa W.: Effect of NaOH content on hydration, mineralogy, porosity and strength in alkali/sulfate-activated binders from ground granulated blast furnace slag and phosphogypsum. Cement and Concrete Research 132 (2020) 106054.

43. Shi C., Roy D., Krivenko P.: Alkali-Activated Cements and Concretes. C. Shi, D. Roy, P. Krinvenko [ed.]. CRC Press, UK. 2006.

44. Fernández-Jiménez A., Palomo J.G., Puertas F.: Alkali-activated slag mortars: Mechanical strength behaviour. Cement and Concrete Research 29(8) (1999), 1313–1321

45. Palomo A., Maltseva O., Garcia-Lodeiro I., Fernández-Jiménez A.: Portland versus alkaline cement: Continuity or clean break: A key decision for global sustainability. Frontiers in Chemistry (2021) 9 705475.